Journal of Applied Polymer Science

Flame retardancy and crack resistance of transparent intumescent fire-resistive coatings

Ling Hong, Xiaoxian Hu, Weiwei Rao, Xiaoping Zhang
Department of Chemistry, School of Science, Shanghai University, Shanghai, China
Correspondence to: L. Hong (E-mail: hongl99@shu.edu.cn)

ABSTRACT: In this article, dihydroxy polydimethylsiloxane ($n = 5–10$) was introduced into the structure of polyphosphate (PPE) to get siloxane-modified polyphosphate (SiPPE). Five kinds of SiPPEs with different Si contents were obtained. FTIR (Fourier Transform Infrared spectroscopy) ICP (Inductively Coupled Plasma Emission Spectroscopy), ^{31}P NMR (Nuclear Magnetic Resonance Spectroscopy) and TGA (Thermogravimetric Analysis) were used to characterize the composition and structure of PPE and SiPPEs. Six kinds of transparent fire-resistive coatings were prepared by the mixing of amino resin with PPE and five kinds of SiPPEs. The results of the fire protection test showed that both the fire-resistive time of coatings and intumescent factor of char layers increased with the increase in content of Si. The results of TGA demonstrated that the carbonaceous residue of coating also increased regularly. The hardness, flexibility, digital photos, SEM (Scanning Electronic Microscopy) and other testing results showed that the introduction of silicon oxygen segment can effectively improve the crack resistance. The charcoal layer structure was more solid than before and collapse was not obvious after long time flame shock. © 2015 Wiley Periodicals, Inc. J. Appl. Polym. Sci. **2015**, *132*, 42423.

KEYWORDS: coatings; degradation; morphology; polyesters; thermal properties

Received 28 October 2014; accepted 26 April 2015
DOI: 10.1002/app.42423

INTRODUCTION

In the recent years, intumescent fire-resistive coatings have been widely used for effective fire protection for various kinds of materials. When encountering flame or high temperatures, intumescent fire-resistive coating can foam and the foamed char layer serves as a superior protective barrier to the main material against flame and heat.[1,2] Some facilities such as ancient buildings, high-class furniture, and architectural decorations need to maintain their original appearance when being coated. Therefore, the development of novel transparent fire-resistive coatings should be given great attention.

The phosphorus-containing polymers are of great interest for transparent fire-resistive coatings due to many advantages. Firstly, they contain both carbon source and acid source, which are necessary to form an effective char layer. Secondly, they are reacted with matrix resin and will not exude from polymer materials during use.[3,4] Finally, the transparency of cured coats will be not greatly affected. Phosphorus-containing polymers decompose at a lower thermal temperature than that of the substrate because of the weak bonds of phosphorate. They form a surface layer protective char during fire before the substrate materials begin to decompose.[5–8] The nitrogen-containing compounds produce incombustible gases without toxic smoke and fog when decomposing at high temperature. The gases can dilute the concentration of the oxygen near the flame. The action of the evolved gases could foam the protective layer while heating. The foamed char layers serve as superior protective barriers to the substrate material against flame and heat.[9]

The silicon-containing compounds can migrate onto the surface of the material during the thermal degradation course because of their low surface energy. Their products are silica carbon with high thermal stability. Silicon carbide can form a protective silica layer and protect the polymer residue from further thermal decomposition at high temperature.[10]

In our previous research,[11] polyphosphates (PPEs) were synthesized from polyphosphoric acid, polyol, and different length of polyethylene glycol (PEG). The introduction of PEG chain can effectively improve the flexibility of the coating. But the fire-resistive time of the coating and the intumescent factor of char layer decreased with the increase of molecular weight of PEG. In this article, organic siloxane was introduced into the structure of PPE to get siloxane-modified polyphosphate (SiPPE). Five kinds of SiPPEs with different of Si contents were obtained. The transparent fire-resistive coatings were prepared by the mixing of amino resin (AR) with PPE or SiPPEs. The chemical structure and composition of PPE and SiPPEs were characterized by FTIR ICP, ^{31}P NMR, and TGA. Their fire protection performance was investigated through fire protection test. In

addition, the thermal degradation behavior, crack resistance as well as the morphology and structure of the char layers were studied by TGA, digital photos, SEM, and other testing methods.

EXPERIMENTAL

Materials

Polyphosphoric acid (PPA), Pentaerythritol (PER), 1,3-Butanediol (BG), isobutyl alcohol, and PEG400 (molecular weight 400) were supplied by Sinopharm Chemical Reagent Co., Ltd., China. AR (model 5718) was supplied by Shanghai Ailijin Coating Co., Ltd., China. α,ω-Dihydroxy polydimethylsiloxane (Hy-siloxane, $n = 5–10$) was purchased from Wuxi Quanli Chem. Co., Ltd., China. All reagents were used as received without further purification.

Synthesis of PPE and SiPPEs

PPA (0.2 mol), BG (0.5–0.46 mol), PEG400 (0.1 mol), and PER (0.2 mol) were placed into a 500 mL four neck flask and stirred for 1 h at 50°C. And then the system was kept at a reflux temperature of about 116°C for 4 h. A light yellow transparent viscous liquid product was obtained and named as PPE.

Hy-siloxane ($n = 5–10$) (0.005—0.04 mol) was then slowly poured into the flask and stirred for another 3 h. The H_2O was removed by distillation under reduced pressure. The product was separated into two layers after standing for 4 h. The lower portion was light yellow transparent liquid and it was the SiPPE. Hydroxyl siloxane was incorporated into PPE to form SiPPE. The SiPPEs with different Si content were marked as $SiPPE_1$–$SiPPE_5$, respectively. The upper portion was slightly transparent colorless liquid which contained the self-polymerized siloxane and the unreacted siloxane. It could be easily separated from the SiPPE layer.

Preparation of Transparent Coatings

Forty-five grams of PPE or SiPPE isobutyl alcohol solution (50% wt) and 90 g AR isobutyl alcohol solution (60% wt) were mixed well. The obtained mixture was painted on tinplate (12 cm × 2.5 cm × 0.02 cm) or plywood board (10 cm × 10 cm × 0.35 cm) with paint brush and the amount was 500 g/m^2. The coating cured to 0.4 mm thick film at room temperature. The coatings made from PPE and $SiPPE_1$–$SiPPE_5$ were named as AS0B and AS1B–AS5B, respectively.

Measurement and Characterization

FTIR was carried out by Nicolet AVATAR 370 FTIR spectrometer (Nicolet Co., American). ^{31}P NMR measurement was conducted on a MERCURY plus 400 spectrometer (Varian, Inc., USA) at room temperature with acetone as the solvent. STA409PC TGA analyzer (Netzsch Co., Germany) was used for the TGA analysis and performed from 30°C to 800°C at heating rate of 20°C/min under nitrogen gas (50 mL/min). The Si content of SiPPE was measured by ICAP 6300 inductively coupled plasma emission spectrometry (ICP, Thermo-Fisher Scientific, England).

The hardness of the coatings was analyzed according to ASTM D3363-05. The flexibility of supported coating films (on tinplates) was carried out by mandrel bend according to standard GB/T 1731-1993. The Adhesion property of the coatings was measured according to ASTM D3359-09. The crack resistance property of the coating films painted on tinplates was shown through digital photos.

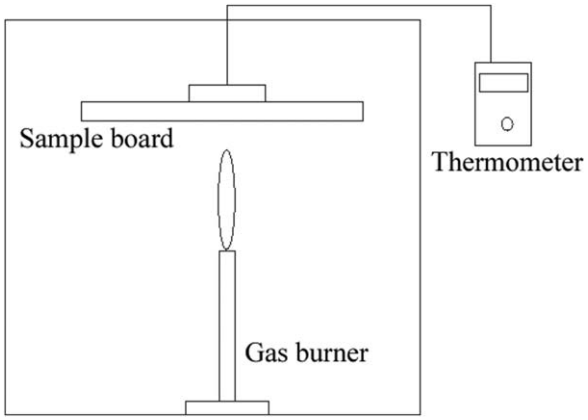

Figure 1. Equipment for fire protection test.

The morphological structure and the distribution of the cell size of the char layers were observed using a JSM-6700F device (JEOL Ltd., Japan) and digital photos.

Fire Protection Test

The fire protection test was carried out using the equipment shown in Figure 1. The side of the plywood board coated with a transparent coating was exposed to the gas burner and burned until the temperature of the backside of the sample board reached 220°C. During the test, the temperature of the backside of the sample board was recorded by digital thermometer and drawn as a function of time.

RESULTS AND DISCUSSION

Synthesis and Characterization of PPE and SiPPEs

PPE was achieved by the esterification between PPA and BG, PEG400, and pentaerythrito. Hy-siloxane was introduced into the structure of PPE by the reaction of the hydroxyl in Hy-siloxane and P–OH, C–OH groups in PPE. The possible reaction formula of PPE and SiPPE was shown in Scheme 1. Five different SiPPEs with different content of Hy-siloxane were synthesized. Different reaction compositions were set and the calculation results of Si content in SiPPEs (Si (wt %)-Cal) are shown in Table I.

The actual values of Si content in SiPPEs measured by ICP (Si ((wt %)-ICP) are also listed in Table I. As can be seen, the Si content of the $SiPPE_3$ has the highest Si content, 0.135%, followed by 0.118% for $SiPPE_2$ and 0.102% for $SiPPE_4$. Initially, the actual Si content increased with the increasing amount of hydroxyl siloxane, but the Si content decreased with the further increasing in the amount of hydroxyl siloxane. This may due to the fact that the self-polymerization of hydroxyl siloxane increased with its increasing content in the polymerization system.[12]

PPE, Hy-siloxane, and $SiPPE_3$ were measured by FTIR to analyze the structure and the results are shown in Figure 2. The absorption observed around 3300 cm^{-1} was attributed to the

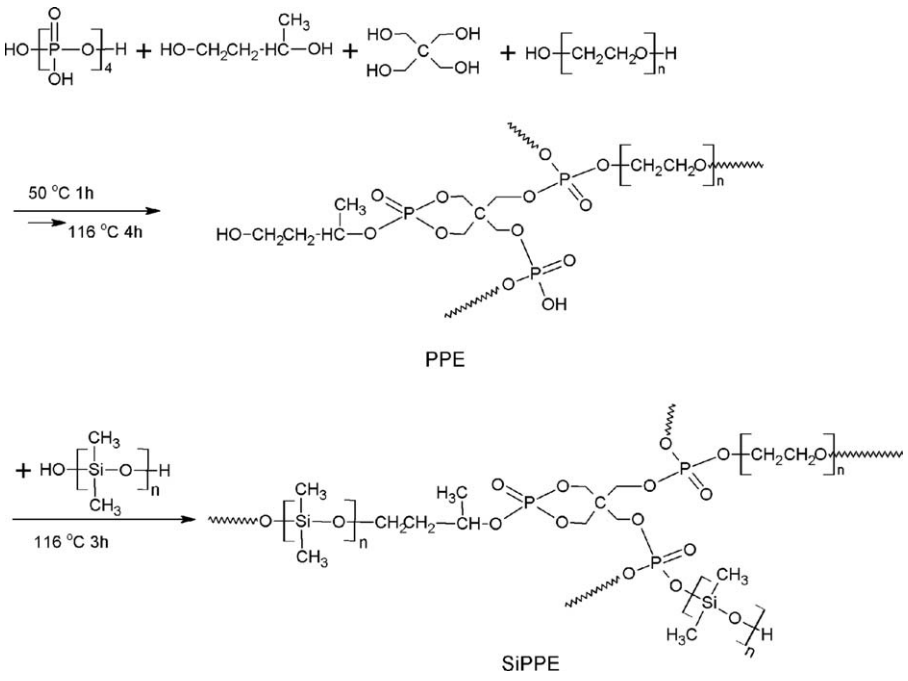

Scheme 1. Reactions of PPE and SiPPE.

vibration absorption of –OH in Si–OH group, and the absorption at 3350 cm^{-1} was for –OH of C–OH group in the PPE. The absorption of –OH bond shifted to 3405 cm^{-1} in the $SiPPE_3$. The peaks at 2350 cm^{-1} were attributed to the absorption of P–O–H bond. The peaks at 2948 and 2887 cm^{-1} were attributed to the vibration absorption of $–CH_3$ and $–CH_2$ groups, respectively. The Si–O–Si group can be detected in the $SiPPE_3$ at 1100–1080 cm^{-1}.[13,14] Combining the analysis of ICP, it indicated the reaction of Si–OH with P–OH and C–OH. The possible reaction formula of the PPE and SiPPE is shown in Scheme 1.

^{31}P NMR was used to analyze the structures of the PPE and $SiPPE_3$. The results are shown in Figure 3. The chemical shift from −0.72 to −0.88 ppm was attributed to the exocyclic P atoms. The chemical shift at about −4.21 ppm was attributed to the P atoms in the cyclic structure.[3] The integral ratio of these two areas is 11 : 1. When $HO[Si(CH_3)_2]_nOH$ ($n = 5–10$) was introduced, the chemical shift of two kinds of P atoms changed distinctly in the ^{31}P NMR spectra of $SiPPE_3$. The peak at about −4.21 ppm could almost be ignored. The peak number and peak shape from −0.72 to −0.88 ppm is obviously different from those of the PPE, and it indicated the reaction between P–OH and Si–OH groups.

Thermal Degradation Behavior of PPE and $SiPPE_3$

The thermal degradation behavior of PPE and $SiPPE_3$ were investigated by TGA. The results are shown in Figures 4 and 5. It can be seen that the whole thermal degradation progress could be divided into several stages.[15–17] In the first stage (50–180°C), the main changes were considered to be the scission of P–O–C bond. The weight losses of PPE and $SiPPE_3$ were almost the same, about 3.2%. In the second stage (180–300°C), PPE lost 31.0% and $SiPPE_3$ lost 24.7%. This weight loss was considered to be the destruction of the P–O–C bond, thus phosphoric acid moieties were liberated. In this stage, the weight loss of $SiPPE_3$ was far less than PPE. From this result, it seemed that the introduction of Hy-siloxane could reduce the destruction of P–O–C bond at this temperature stage. When the temperature reached 300–480°C (the third stage), PPE lost 13.6% and

Table I. The Composition of the PPE, SiPPEs, and the Data of ICP

		Mole ratio of	
Sample	PPA/PER/PEG400/BG/Hy-silane	Si (wt %)-Cal	Si ((wt %)-ICP
PPE	0.2/ 0.2/ 0.1 /0.5 / --	0	0
$SiPPE_1$	0.2/ 0.2/ 0.1/ 0.495/ 0.005	0.52	0.098
$SiPPE_2$	0.2/ 0.2/ 0.1/ 0.49/ 0.01	1.03	0.118
$SiPPE_3$	0.2/ 0.2/ 0.1/ 0.48/ 0.02	2.01	0.135
$SiPPE_4$	0.2/ 0.2/ 0.1/ 0.47/ 0.03	2.94	0.102
$SiPPE_5$	0.2/ 0.2/ 0.1/ 0.46/ 0.04	3.82	0.075

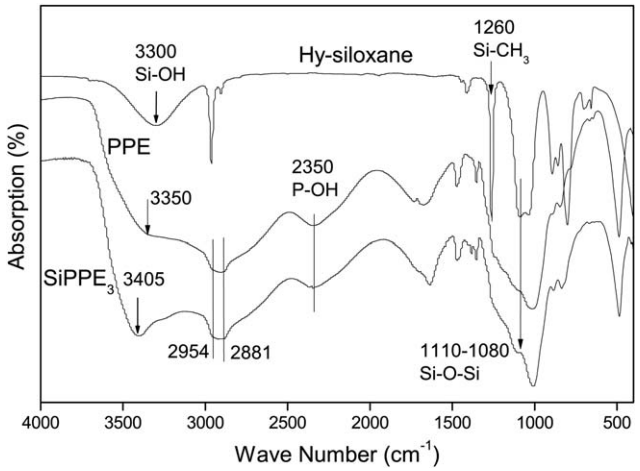

Figure 2. FT-IR spectrum of PPE, Hy-siloxane, and $SiPPE_3$.

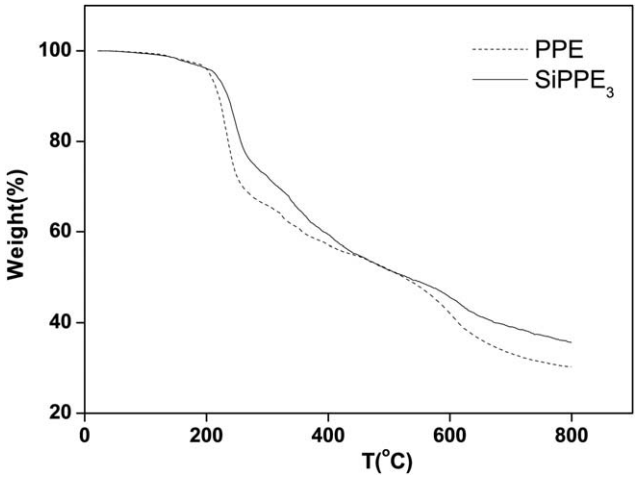

Figure 4. TGA curves of PPE and $SiPPE_3$.

$SiPPE_3$ lost 19.2%. They kept decomposing and liberated an abundance of phosphoric acid and char layer began to be formed. When the temperature further went up to the fourth stage (above 480°C), unstable carbon-containing structures were decomposing to release CO and CO_2 and final char layer was formed. The final residue weight of PPE and $SiPPE_3$ were 30.3% and 34.2%, respectively. Above all, $SiPPE_3$ had higher stability than PPE at high temperature, and Si could make a contribution to the carbonaceous residue formation.

Crack Resistance of the Coatings

Six kinds of novel transparent fire fire-resistive coatings (AS0B–AS5B) were prepared by mixing PPE or $SiPPE_1$-$SiPPE_5$ with AR. Figure 6 shows the appearance of the coatings based on tin plate after 3 months at room temperature. The AS_0B film, not modified by siloxane, was curled wrinkling, cracking, and peeling. The crack resistance property was improved when the siloxane was incorporated into PPE. With the increasing of the Si content in the polymer, the wrinkles and spalling of the film decreased. The AS3B coating has the highest Si content and it showed the best crack resistance property. This indicated that Si–O chains can effectively improve the performance of crack resistance.

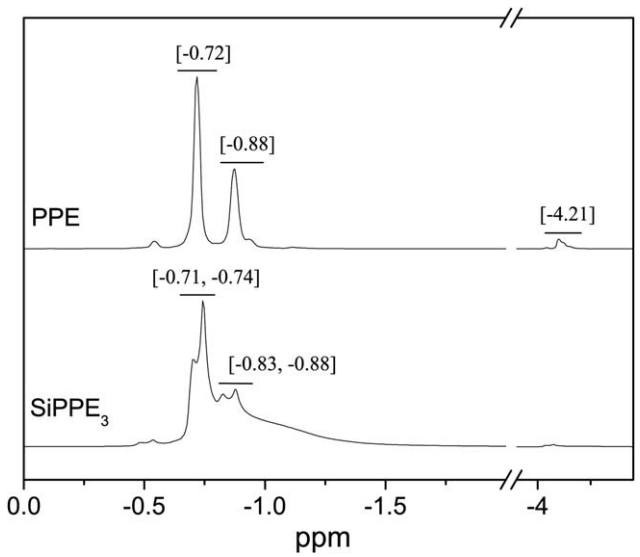

Figure 3. ^{31}P NMR spectrum of PPE and $SiPPE_3$.

Fire Protection Property of the Coatings

Fire protection is the key performance criteria for fire-resistive coatings. The backside temperature of sample board could be observed and plotted as a function of time through fire protection test. The results of the fire protection test for the six coatings are shown in Figure 7. The intumescent factors (the ratio of thickness before and after burning) of coatings are also showed in Figure 8.

From Figure 7, it can be noted that the backside temperature of the blank board increased rapidly and reached 220°C within 2 min. The backside temperature of all the coated boards increased rapidly to about 155–187°C at the first 4 min. Then they all decreased a little and presented a relatively equilibrium state, which was maintained almost unchanged for a long time when the coatings swelled to the maximum. The multiporous char structure caused by expansion on the front surface hampered the heat transfer to the back surface. The backside

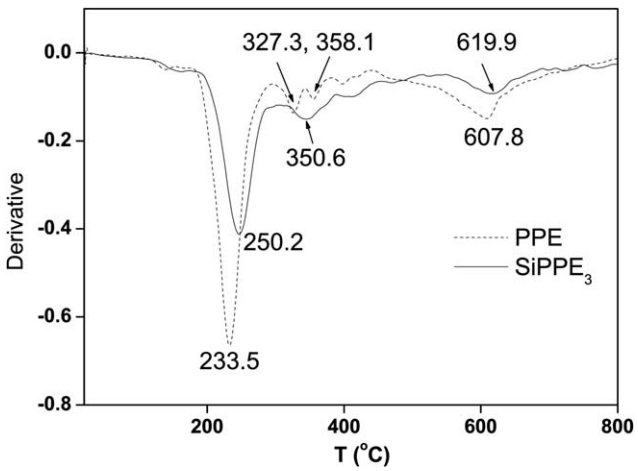

Figure 5. DTG curves of PPE and $SiPPE_3$. [Color figure can be viewed in the online issue, which is available at wileyonlinelibrary.com.]

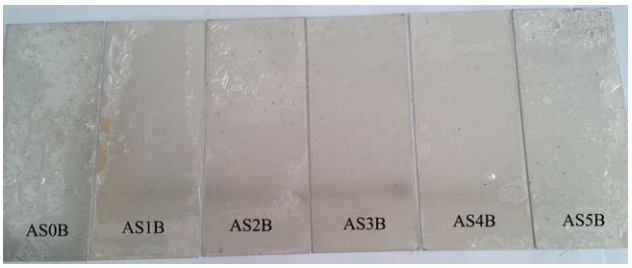

Figure 6. Digital photo of coatings after 3 months at room temperature (base: tin plate). [Color figure can be viewed in the online issue, which is available at wileyonlinelibrary.com.]

temperature then increased again at the end of the equilibrium state and reached 220°C within several minutes. This might be due to the fact that cracks and collapse appeared in the intumescent carbon layer after long time burning.

Here we define the needed time, which the backside temperature of sample boards reached 220°C as fire-resistive time. From Figure 7, it can be seen that the fire-resistive times for blank board, AS0B, and AS1B–AS5B were 1.9, 33.4, 35.9, 38.8, 41.6, 36.8, and 34.6 min, respectively. It could be concluded that the thermal barrier effect of intumescent coatings increased with the increase of the Si content. Long fire-resistive time also means good fire retardancy. The fire-resistive time of each AS1B–AS5B sample was longer than that of AS0B, showing that the coatings prepared by SiPPEs could indeed offer better fire protection for wood board. It was obvious that the Si content in the SiPPE had a regular influence on the fire retardancy of coatings. The AS3B sample had the highest intumescent factor and showed the best fire retardancy due to its highest Si content.

Thermal Degradation Behavior of the Coatings

TGA was employed to observe the thermal degradation behavior of the six coatings and the results are shown in Figure 9. It can be seen from the curves that the thermal decomposition was carried out step by step. Under 150°C, the mass loss was mainly caused by dehydration.

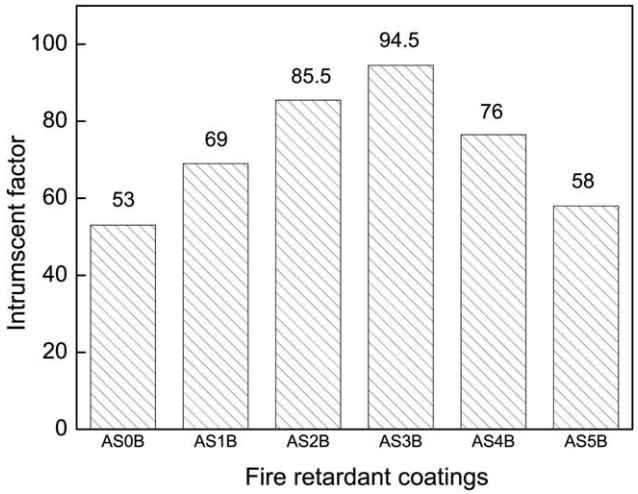

Figure 8. Intumescent factors of coatings.

The mass loss rate became faster at 250–480°C and it was caused by the degradation of phosphate and the decomposition of ammonia. This can enhance the flame retardancy of the coating polymer because that the degraded products of phosphate unit have great contributions to the formation of phosphorus-rich cross-linking carbonization char during expansion process.[18–20] The obtained intumescent char acted as a protective layer on the substrate surface against heat and diffusion of oxygen and prevented the further thermal decomposition.

As a result, when the temperature was much higher, the coating with higher content of Si was more stable and yields more char after degradation. For example, the weight loss at 480–800°C was about 13% for AS3B, 15–16% for AS2B, AS4B, and AS1B, 18% for AS5B, but 25% for AS0B. The final residue weights of AS0B–AS5B were 9.34%, 15.13%, 23.03%, 27.31%, 19.90%, and 12.68%, respectively. The coating with higher Si content showed a less degradation at high temperature, and the char residue increased. It could probably be attributed that the Si–O chains would contribute to forming a more stable char residue

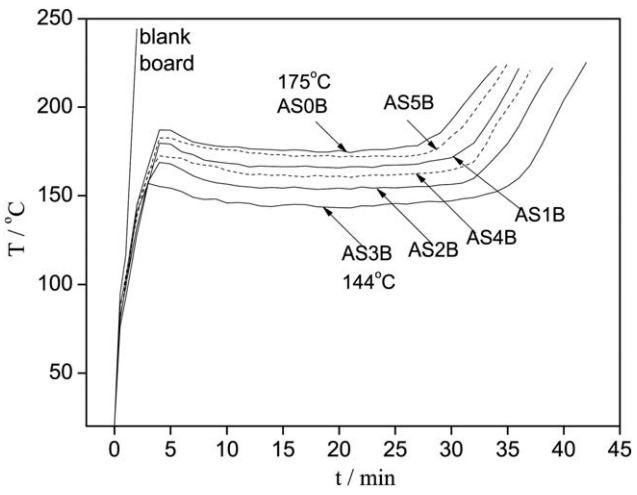

Figure 7. Backside temperature–time curves of the boards.

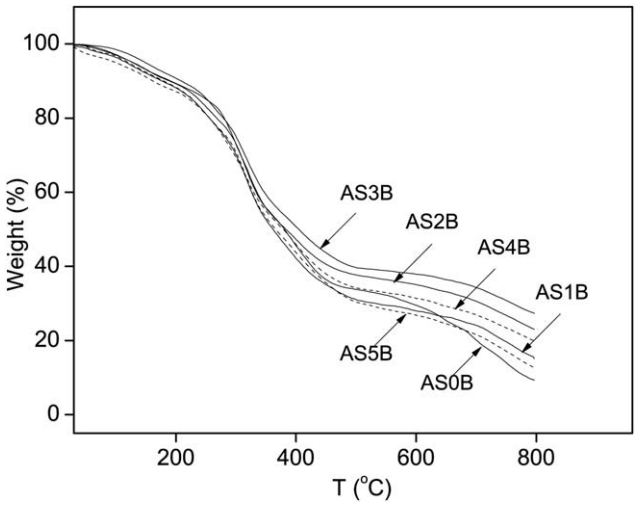

Figure 9. TGA curves of the coatings.

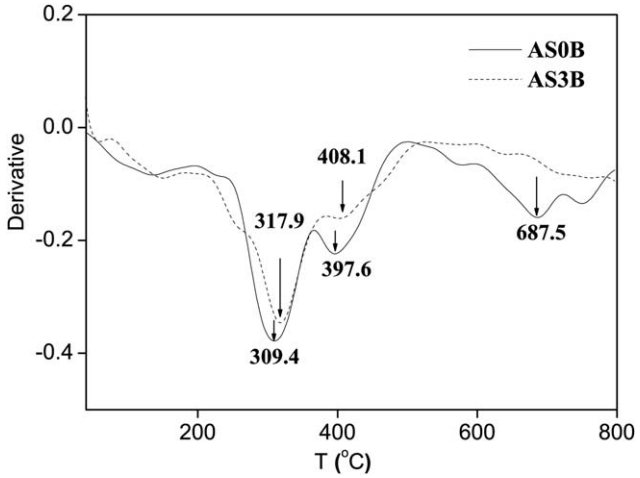

Figure 10. DTG curves of the coatings. [Color figure can be viewed in the online issue, which is available at wileyonlinelibrary.com.]

structure. The AS0B sample containing no Si–O chain was easily decomposed to CO and CO_2 at high temperature.

Figure 10 shows the DTG (Derivative Thermogravimetry) curves for AS0B and AS3B. It can be seen that the whole thermal degradation progress could be divided into three stages. In the first stage (50–151°C), the main changes were considered to be the dehydration. When the temperature rose sequentially and reached 250–480°C (the second stage), the coatings kept decomposing and liberated an abundance of phosphoric acid. This phosphoric acid catalyzed the cleavage of carbonyl groups to form more stable polynuclear structure and char layer began to be formed. There were two peaks in this stage, 309.4°C and 397.6°C for AS0B, and 317.9°C and 408.1°C for AS3B. The maximum degradation temperature of AS0B was lower than that of AS3B. At the same time, the weight loss of AS0B was bigger than that of AS3B.

When the temperature further went up to the third stage (above 480°C), unstable carbon-containing structures were decomposing to release CO and CO_2 and final char layer was formed. The weight loss of AS0B was far higher than that of AS3B, indicating that the Si–O containing structure was stable at high temperature.

Morphological Structure of Intumescent Char Layers

The efficiency of char layer depends strongly on its foam structure and surface morphology.[21] Figure 11 shows the digital photos of the coatings which expanded to the maximum. All the coating could form a dense, homogeneous layer of sponge-like carbon after combustion. These would be a benefit for fire insulation in the combustion process. However, the intumescent factors of each coating were different (Figure 8). The intumescent factors for AS3B and AS2B reached 94.5% and 84.5% separately. They were significantly higher than 53% for AS0B.

The carbon layer morphologies of AS1B–AS5B were also significantly different from AS0B sample which did not contain silicon. The carbon layer of AS0B was black, while samples containing Si were slightly gray. The middle part of AS0B showed a slight depression due to flame shock, but the middle parts of AS1B, AS2B, and AS3B were the highest part in the

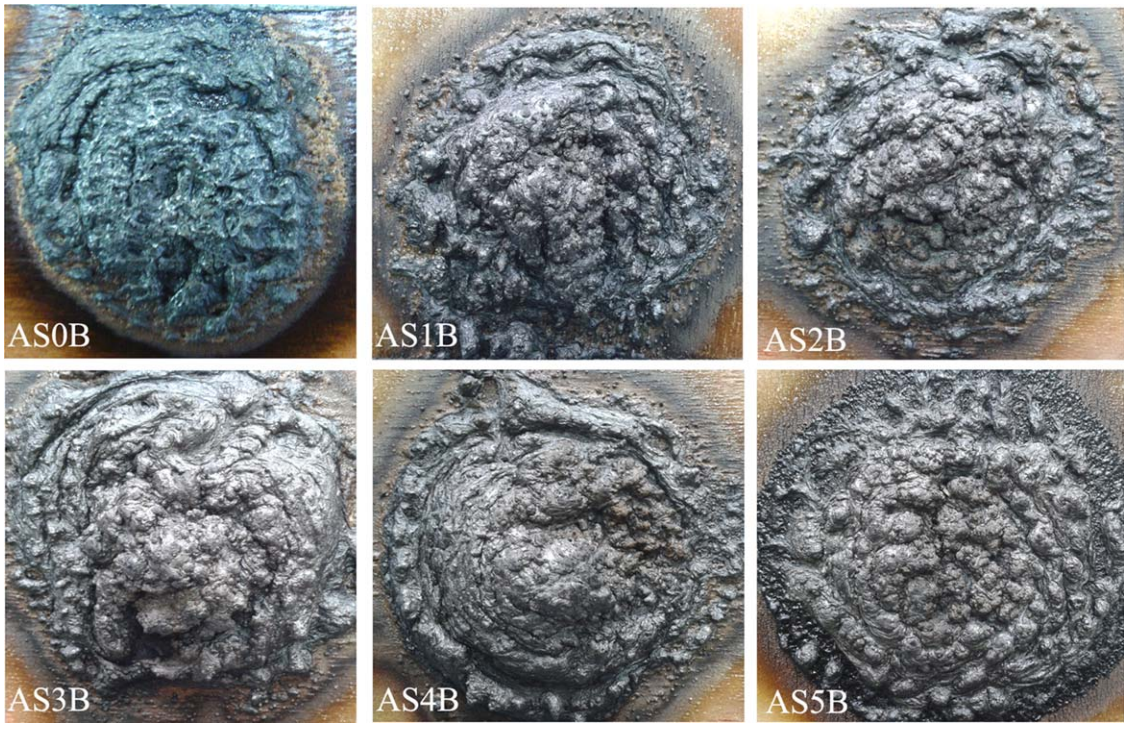

Figure 11. Digital photos of specimen coatings after burning. [Color figure can be viewed in the online issue, which is available at wileyonlinelibrary.com.]

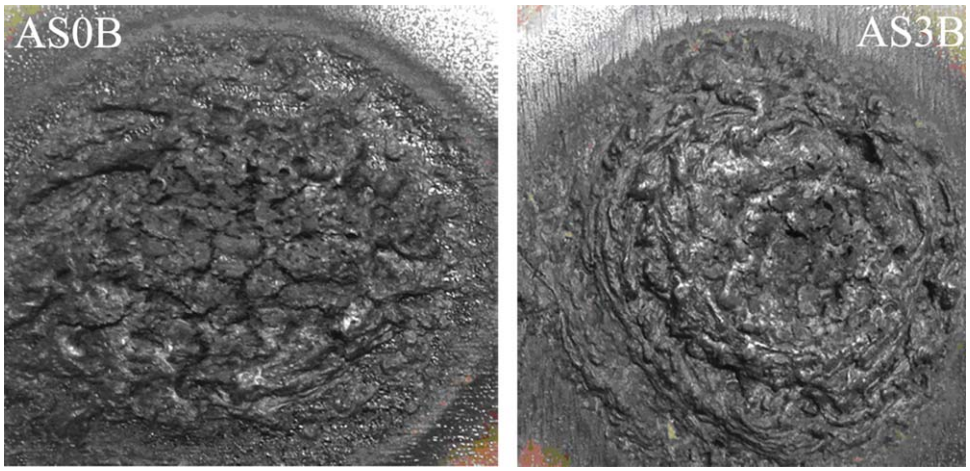

Figure 12. Digital photos of specimen coatings after burning 30 min. [Color figure can be viewed in the online issue, which is available at wileyonlinelibrary.com.]

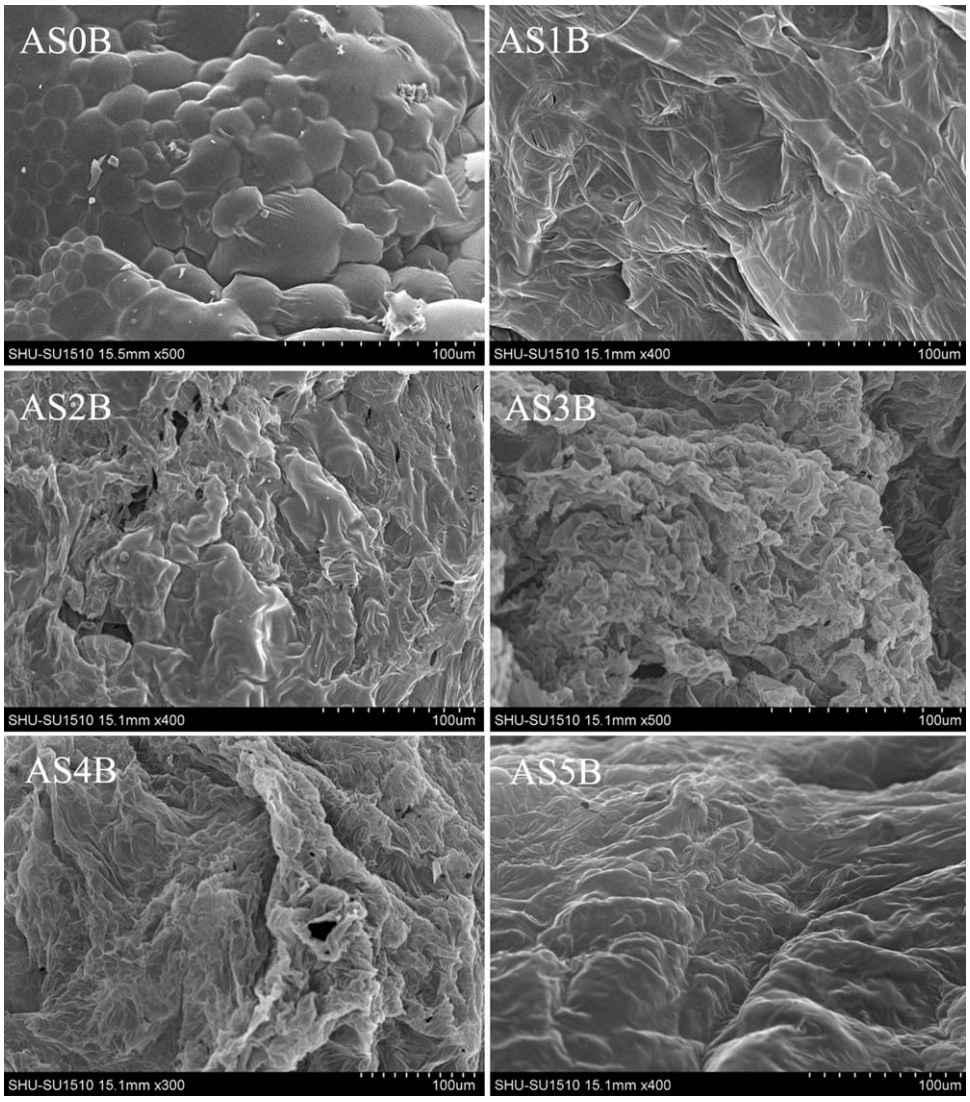

Figure 13. SEM micrographs of the surface of the char layers.

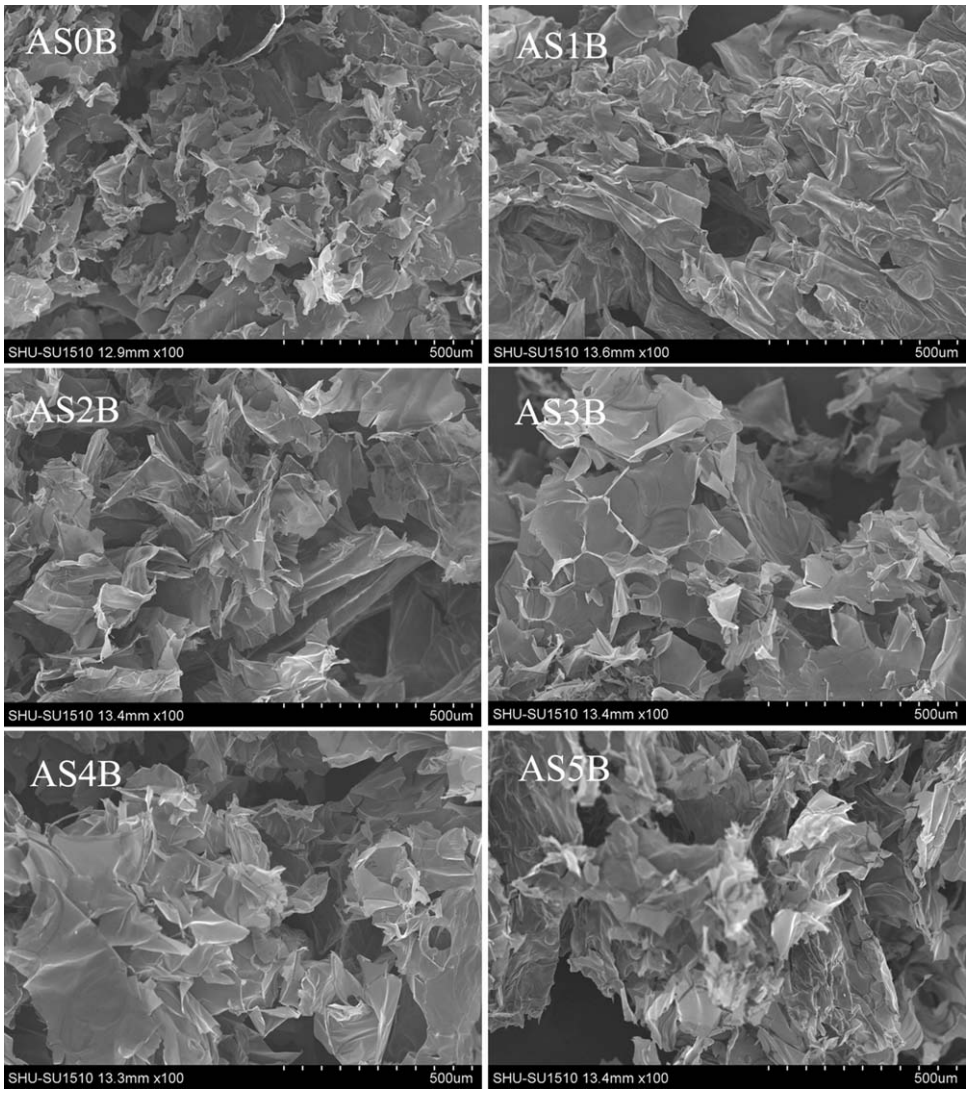

Figure 14. SEM micrographs of the internal of the char layers.

layer under the flame impingement. This indicated that the carbon layer structure containing Si was more solid.

Figure 12 also shows the digital photos of AS0B and AS3B after 30 min of combustion. As can be seen, the carbon layer of AS0B would shrink. Collapse and crack appeared under the long time flame shock. The carbon layer of AS3B also shrinked, but the general structure remained intact. The carbon layer containing silica segment was more stable.

The morphological structure of the outside and the inside of the carbon layer were observed by SEM and the results are shown in Figures 13 and 14, respectively. The surface of AS0B carbon layer showed bubble-like structure and the surface was relatively intact. The surface expansion structures were obvious for AS2B, AS3B, and AS4B. The expansion for AS3B was the most prominent and it indicated that the charcoal layer had the most porous structure, which could effectively prevent the heat transferring to the wood board, thus providing good fire-resistive protection. This result was in accordant with the previous experimental phenomenon.

Figure 14 was the SEM micrographs of the internal of the char layers. The internal carbon layer showed expanded loose sheet structure. Between the sheets was filled with gas produced in

Table II. Hardness, Flexibility and Adhesion of the Coatings

Performance	AS0B	AS1B	AS2B	AS3B	AS4B	AS5B
Pencil Hardness	4H	4H	5H	5H	5H	5H
Flexibility/mm	>15	>15	15	10	10	>15
Adhesion Classification	3B	3B	3B	3B	3B	3B

the decomposition process, so that the heat conduction was blocked and the temperature rise slowed down. It could be seen that the sheets in AS3B, AS2B, and AS4B were large and uniform. The holes between sheets were large too. The sheets in AS0B were small and nonuniform. The porous structures of AS_1B and AS_5B were less obvious than those of AS2B–AS4B. Large and uniform sheet structure had good ability to support its carbon layer, and deformation was not easy to occur under flame shock. This would help to improve the flame retardant time.

Hardness, Flexibility, and Adhesion of the Coatings

The hardness, flexibility, and adhesion of the coatings are listed in Table II. The hardness of AS2B–AS5B increased a little to 5H from 4H of AS0B. The value of the flexibility was 10 mm for AS3B and AS4B and >15 mm for AS0B. The coatings containing higher content of Si–O chain showed more flexible property. It indicated that the introduction of Si–O chain can increase flexibility. But the Si–O chain had little influence on the adhesion of the coatings.

CONCLUSIONS

In this work, PPE was synthesized by the reaction of PPA, PER, and PEG400. In order to improve the flame retardancy and crack resistance of transparent fire-resistive coatings, organic siloxane was introduced in the structure of PPE to obtain SiPPEs. Initially, the actual Si content increased with the increasing amount of hydroxyl siloxane, but the Si content decreased with the further increasing in the amount of hydroxyl siloxane due to the self-polymerization of hydroxyl siloxane.

Six kinds of novel transparent fire-resistive coatings (AS0B–AS5B) were prepared by mixing PPE or $SiPPE_1$–$SiPPE_5$ with AR. The coating with higher Si content showed the better crack resistance property. This indicated that Si–O chains can effectively improve the performance of crack resistance.

From the fire protection test, it could be seen that the coatings had effective protection for the wood board, and both the fire-resistive time and intumescent factor of char layers increased with the increase of Si content. Hence, the AS3B coating prepared from $SiPPE_3$ had best fire retardancy. Its fire-resistive time could reach 41.5 min and intumescent factor achieved 94.5. The result of TGA showed the thermal stability of coatings also increased regularly with the increase of Si content.

The carbon layer structure containing Si was more solid, which would not be easy to shrink and collapse. The expansion for AS3B was the most prominent and the internal of the char layers contained large and uniform sheets. The porous structure could effectively prevent the heat transferring to the wood board, thus providing good fire-resistive protection.

REFERENCES

1. Xing, W. Y.; Zhang, P.; Song, L.; Wang, X.; Hu, Y. *Mater. Res. Bull.* **2014**, *49*, 1.
2. Camino, G.; Lomakin, S. In Fire Retardant Materials, Horrocks, A. R., Price, D., Eds.; Woodhead Publishing: Cambridge, **2001**; p 318.
3. Hu, X.; Wang, G. J.; Huang, Y. *J. Coat. Technol. Res.* **2013**, *10*, 717.
4. Price, D.; Pyrah, K.; Hull, T. R.; Milnes, G. J.; Wooley, W. D.; Ebdon, J. R.; Hunt, B. J.; Konkel, C. S. *Polym. Int.* **2000**, *49*, 1164.
5. Lu, S. Y.; Hamerton, I. *Prog. Polym. Sci.* **2002**, *27*, 1661.
6. Li, Q.; Jiang, P.; Su, Z.; Wei, P.; Wang, G.; Tang, X. *J. Appl. Polym. Sci.* **2005**, *96*, 854.
7. Chiang, C. L.; Chang, R. C.; Chiu, Y. C. *Thermochim. Acta* **2007**, *453*, 97.
8. Chiang, C. L.; Ma, C. C. *Polym. Degrad. Stabil.* **2004**, *83*, 207.
9. Zaikov, G. E.; Lomakin, S. M. *Polym. Degrad. Stabil.* **1996**, *54*, 223.
10. Chiang, C. L.; Chang, R. C. *Compos. Sci. Tech.* **2008**, *68*, 2849.
11. Hu, X. X.; Hong, L. *Paint Coat. Indus. (in Chinese)* **2013**, *43*, 42.
12. Xu, Z. Y. Siloxane-modified polyester: synthesis and features of its powder coating, Dissertation for Master Degree, Zhejiang University, China, **2003**, 27.
13. Renier, M. L.; Kohn, D. H. *Biomed. J. Mater. Res.* **1997**, *34*, 95.
14. Chen, Y. W.; Chuang, J. R.; Yang, Y. C.; Li, C. Y.; Chiu, Y. S. *J. Appl. Polym. Sci.* **1998**, *69*, 115.
15. Guo,Y. N.; Ming, J. Y.; Li, C. Y.; Qiu, J. J.; Tang, H. Q.; Liu, C. M. *J. Appl. Polym. Sci.* **2011**, *121*, 3137.
16. Gu, G.; Li, X. *Chem. Build. Mater.* (in Chinese) **2003**, *6*, 14.
17. Wang, G.; Huang, Y.; Hu, X. *Prog. Org. Coat.* **2013**, *76*, 188.
18. Liu, Y. L.; Hsiue, G. H.; Lan, C. W.; Chiu, Y. S. *J. Polym. Sci., Part A: Polym. Chem.* **1994**, *35*, 565.
19. Wang, H.; Wang, Q.; Huang, Z.; Shi, W. *Polym. Degrad. Stab.* **2007**, *92*, 1788.
20. Li, S. F.; Wang, H. L.; Tao, M. *Des. Monomers Polym.* **2014**, *17*, 693.
21. Wang, Z.; Han, E.; Ke, W. *Surf. Coat. Technol.* **2006**, *200*, 5706.